


Article

Assessment of the Harmonics Influence on the Power Consumption of an Electric Submersible Pump Installation

Aleksandr Lyakhomskii ¹, Anton Petrochenkov ^{1,2,*} , Aleksandr Romodin ², Evgenia Perfil'eva ¹, Sergey Mishurinskikh ², Andrei Kokorev ², Aleksandr Kokorev ² and Sergei Zuev ²

¹ College of Mining, National University of Science and Technology MISIS, 119049 Moscow, Russia; lav5723807@mail.ru (A.L.); mgggu.eegp@mail.ru (E.P.)

² Electrical Engineering Faculty, Perm National Research Polytechnic University, 614990 Perm, Russia; romodin_av@pstu.ru (A.R.); mishurinskikh_sv@msa.pstu.ru (S.M.); kaa19.77@mail.ru (A.K.); kok881@yandex.ru (A.K.); luckyvoice@yandex.ru (S.Z.)

* Correspondence: pab@msa.pstu.ru; Tel.: +7-3422391821

Abstract: Oil production is a complex technological process that requires significant electricity consumption. The main electricity consumers in oil and gas production workshops are artificial lift facilities. Currently, among the objects of mechanized mining, installations of electric submersible pumps are widespread. When planning technological modes, it is necessary to be able to assess the change in the power consumption parameters when changing the technological process parameters. The paper proposes a typical replacement scheme for the electrical complex element. The power consumption calculation of electric submersible pump installations has been carried out. The error in the power consumption modeling results of electric submersible pump installations in comparison with the results of instrumental measurements is no more than 10%. The estimation of additional losses of electric energy caused by the influence of harmonics is carried out. The proposed technique makes it possible to estimate the power consumption of an electric submersible pump installation when changing the parameters of the technological process and equipment. The results of the work can be used for planning material support and optimization of warehouse stocks within the framework of integrated logistics support for the technological process of industrial enterprises.

Keywords: power consumption; submersible electric motor; electric submersible pump; harmonics



Citation: Lyakhomskii, A.; Petrochenkov, A.; Romodin, A.; Perfil'eva, E.; Mishurinskikh, S.; Kokorev, A.; Kokorev, A.; Zuev, S. Assessment of the Harmonics Influence on the Power Consumption of an Electric Submersible Pump Installation. *Energies* **2022**, *15*, 2409. <https://doi.org/10.3390/en15072409>

Academic Editors: Vladimir Prakht, Federico Barrero, Anton Rassölnkin, Levon Gevorgov, Emilia Iakovleva and Irina Kirpichnikova

Received: 30 January 2022

Accepted: 18 March 2022

Published: 25 March 2022

Publisher's Note: MDPI stays neutral with regard to jurisdictional claims in published maps and institutional affiliations.



Copyright: © 2022 by the authors. Licensee MDPI, Basel, Switzerland. This article is an open access article distributed under the terms and conditions of the Creative Commons Attribution (CC BY) license (<https://creativecommons.org/licenses/by/4.0/>).

1. Introduction

Electricity consumption during oil production is a significant cost item for industry enterprises. When assessing the amount of power consumption, it is necessary to take into account a large number of factors, the majority of which are the technological process parameters and the installed equipment parameters. Currently, in mechanized oil production, installations of electric submersible pumps (ESP) are widely used.

The various authors papers are devoted to the assessment of the ESP power consumption. The studies [1–3] provide a comprehensive description of the ESP power consumption with decomposition by types of equipment; in paper [4], the authors analyzed the existing methods for calculating the ESP power consumption. At the same time, research is being carried out on the individual elements operation of the ESP electrotechnical complex (ETC): the authors of paper [5] considered the issue of the fluid viscosity influence on the electric submersible pump operating characteristics; in papers [6,7], the authors consider the use of permanent magnet motors in enhancement of electric submersible pump; paper [8] is devoted to the use of ultra-high-speed submersible pumps; the issue of optimizing the cross-section of the ESP cable line is considered in paper [9].

The ESP is controlled by a variable frequency drive. Frequency converters in power supply systems are sources of harmonics. Harmonics can have various negative effects on electric equipment, one of which is the additional losses occurrence. The harmonics can be

filtered by harmonics filter and calculation of filter parameters based on harmonic spectrum is presented in paper [10]; in paper [11], the harmonics influence on induction motor losses is considered; paper [12] is devoted to assessing the impact of power quality indices on active power losses in the electric network; a description of systems for measuring and recording electric energy quality indicators is given in papers [13,14]; work [15] presents the application of the equivalent method for calculating the harmonics influence on the parameters of the electrical network functioning; paper [16] presents an approach to electrical energy losses calculation in the main elements of the electrotechnical complex.

Additionally, there is an approach of the pumping plant power's estimation based on Simulink models [17,18]. The one model [17] is developed to provide the possibility of power calculation during both throttling and speed control and can be used for validating power consumption at the design stage of the submersible pump system development. On the other hand [18], the efficiency of the centrifugal pump systems varies significantly with the change of operational point location on the H-Q plane and depends on the positions of the pump and system curves.

Thus, the task of assessing the harmonics influence on the ESP electrical losses includes two aspects: assessing the parameters influence of the electrical and technological modes on power consumption and assessing the effect of harmonics on the number of additional losses.

The developing method for calculating power consumption has to take into account the mutual influence of equipment on power consumption within an oil field when changing the technological process parameters.

2. Materials and Methods

2.1. Research Object

The typical structure of an oil field (OF) ETC is a magistral structure with concentrated loads. In general, the structure of the OF ETC is shown in Figure 1, where: PSS—external power system, T—transformer, OHL—overhead power line, CL—cable power line, SEM—submersible electric motor, ESP—electric submersible pump, CS—control station, IM—induction motor, SR—sucker rod, SL—static load, SS—substation, CTP—complete transformer substation, TO—technological object.

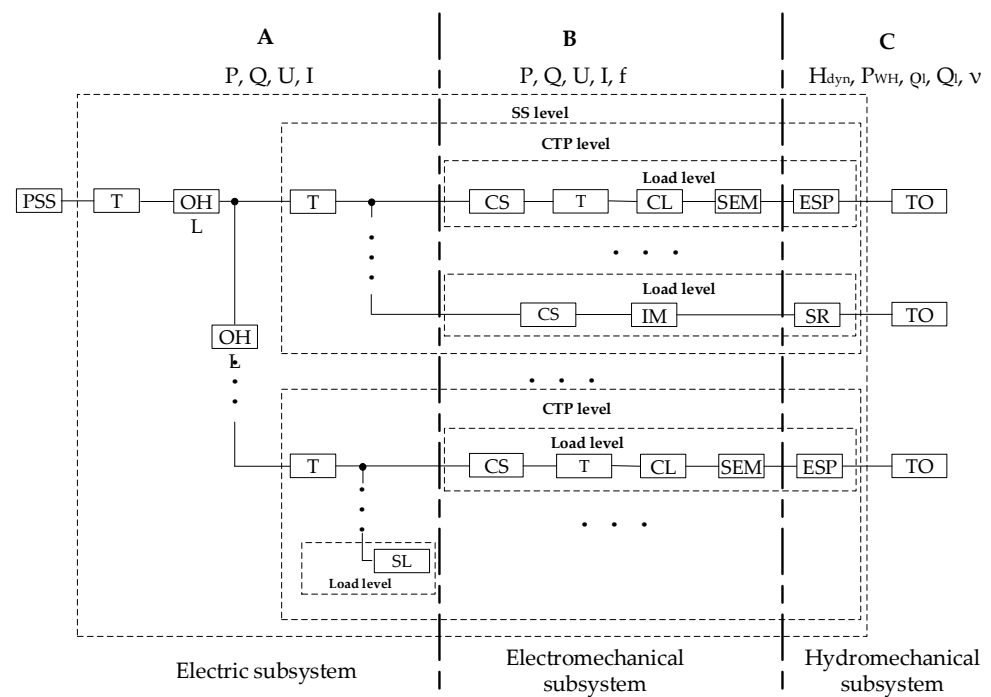


Figure 1. Scheme of OF ETC.

Structurally, OF ETC is divided into 3 levels:

1. Load level (ESP, sucker rod pumping unit (SRPU), SL);
2. The level of the complete transformer substation;
3. Substation level.

The load level is considered as a set of interconnected and interacting subsystems of different physical nature: hydromechanical and electromechanical. This determines the features of modeling the interaction of elements, namely, the list of controlled and observed parameters. To build models, taking into account the peculiarities of their interaction, the OF ETC is divided into three zones:

1. A: oilfield power supply system where no frequency control is performed (electrical subsystem). Controlled parameter—voltage (U (V)); observed parameters: active power (P (W)), reactive power (Q (VAr)), current (I (A));
2. B: electromechanical subsystem of load where frequency and voltage regulation are performed. Controlled parameters—voltage (U (V)), frequency (f (Hz)); observed parameters: active power (P (W)), reactive power (Q (VAr)), current (I (A));
3. C: hydromechanical subsystem of load, where process parameters are controlled by changing the electromechanical subsystem parameters. Controlled parameters: dynamic level (H_{dyn} (m)), wellhead pressure (P_{WH} (Pa)), liquid flow rate (Q_l (m³/day)). Observed parameters: density of the liquid (ρ_l (kg/m³)), viscosity of the liquid (ν (m²/s)). The elements that are not part of the ETC are the working mechanism (ESP, pumping unit) and the technological object—the reservoir. The reservoir is characterized by the properties of the fluid and the energy of the reservoir, which is expressed in the form of reservoir pressure.

2.2. Electrical Mode Parameters Calculation

2.2.1. Electrical Mode Parameters Calculation Method

To calculate the electrical mode parameters, the ETC element model is developed. The element equivalent circuit is shown in Figure 2, where i —the node of the element beginning; j —node of the end of the element; r —the active resistance of the element (Ohm); x —the reactance of the element (Ohm); U_i —voltage at the beginning of the element (V); U_j —voltage at the end of the element (V); ΔP_{const} , ΔP_{var} —constant and variable losses of active power (W); ΔQ_{const} , ΔQ_{var} —constant and variable reactive power losses (VAr).

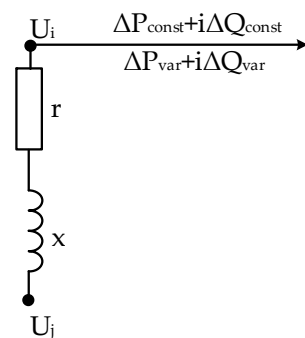


Figure 2. Equivalent circuit of the ETC element.

In most cases, in the oil field the voltage of the substation low voltage buses (which are considered as the apparent power source) and the load power data are available, respectively, and it is possible to calculate the electrical mode parameters iteratively [19].

At the first stage (when $p = 1$), the initial approximation of the consumer voltage \dot{U}_j is set as a nameplate equipment voltage in the load nodes. Based on this approximation, the current value is determined:

$$\dot{I}_{ij}^{(p)} = \frac{P_j - iQ_j}{\sqrt{3} \cdot \dot{U}_j^{(p-1)}}, \quad (1)$$

where p —iteration number.

Then, the found current is substituted into the equation to determine the losses:

$$\Delta \dot{S}_{ij}^{(p)} = \left(\dot{I}_{ij}^{(p)} \right)^2 \cdot \dot{Z}_{ij}, \quad (2)$$

where $\dot{Z} = r + ix$ —complex branch impedance, Ohm.

The power of the apparent power source is determined:

$$\dot{S}_i^{(p)} = \dot{S}_j + \Delta \dot{S}_{ij}^{(p)}. \quad (3)$$

The voltage drop of the element is determined:

$$\Delta \dot{U}_{ij}^{(p)} = \dot{I}_{ij}^{(p)} \cdot \dot{Z}_{ij}. \quad (4)$$

The voltage at the end of the section is determined:

$$\dot{U}_j^{(p)} = \frac{\dot{U}_i^{(p)} - \Delta \dot{U}_{ij}^{(p)}}{K_T}, \quad (5)$$

where K_T —branch transformation ratio.

This cycle is repeated until the difference between certain voltage values at different iterations for load nodes is within the specified error:

$$\left| \dot{U}_j^{(p+1)} - \dot{U}_j^{(p)} \right| < \varepsilon. \quad (6)$$

2.2.2. Calculation Scheme

The interaction scheme of ESP ETC elements is shown in Figure 3 [19,20].

Figure 3 indicates: η_{CS} —control station efficiency; f —the voltage frequency at the control station output; S_{np} —nameplate transformer power; ΔP_T —transformer idle losses; ΔP_{SC} —transformer short circuit losses; U_{HV} —voltage of high voltage windings of transformer; U_{LV} —voltage of low voltage windings of transformer; I_T —transformer idle current; U_{SC} —transformer short-circuit voltage; r_0 —specific active resistance of the submersible cable line; x_0 —the specific reactance of the submersible cable line; l_{CL} —the submersible cable line length; P_{np} —nameplate motor power; U_{np} —nameplate motor voltage; $\cos \varphi (K_L)$ —dependence of the change in the power factor of the SEM on the load factor; $\eta (K_L)$ —dependence of the change in the SEM efficiency on the load factor; Q_{ow} —optimal pump rate of ESP on the water characteristic; $\eta_{ESP} (Q)$ —dependence of the change in the ESP efficiency on the flow rate; Q_{max} —theoretically possible maximum pump flow rate at a head equal to 0 m; P_{ESP} —the power required to drive the ESP; P_{SEM} —active power consumed by the SEM; Q_{SEM} —the reactive power consumed by the SEM; ΔU_{CL} —voltage loss in the cable line; P_{CL} —active power on the HV side of the transformer; Q_{CL} —reactive power on the HV side of the transformer; ΔU_T —voltage loss in the transformer; P_T —active power on the LV side of the transformer; Q_T —reactive power on the LV side of the transformer; P_{ESPI} —active power of ESP installation; Q_{ESPI} —reactive power of ESP installation.

2.2.3. Calculation of ESP Power Consumption

The total electrical power consumed by the ESP installation is determined by the useful power on the motor shaft and the sum of power losses in all circuit elements. According to Figure 3, the total power is determined as [20]:

$$P_{ESPI} = P_{SEM} + \Delta P_{CL} + \Delta P_T + \Delta P_{CS}. \quad (7)$$

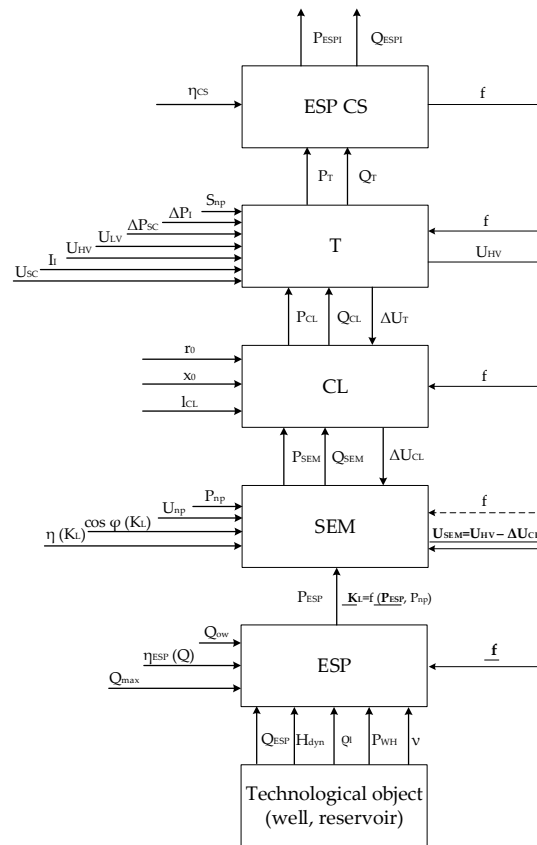


Figure 3. Scheme of interaction of ESP ETC elements.

The power required to drive the ESP is determined by the formula:

$$P_{ESP} = \frac{\rho_l \cdot g \cdot H_{ESP} \cdot Q_{ESP}}{\eta_{ESP} \cdot K_{\eta v} \cdot 86,400} \tag{8}$$

The ESP head is calculated by the formula:

$$H_{ESP} = \left(\frac{P_{WH}}{\rho_l \cdot g} + H_{dyn} \right) \tag{9}$$

ESP efficiency is described by the polynomial [20]:

$$\eta_{ESP} = a_0 + a_1 \left(\frac{50}{f} \right) \cdot \left(\frac{Q_{ESP}}{Q_{max}} \right) + a_2 \left(\frac{50}{f} \right)^2 \cdot \left(\frac{Q_{ESP}}{Q_{max}} \right)^2 + a_3 \left(\frac{50}{f} \right)^3 \cdot \left(\frac{Q_{ESP}}{Q_{max}} \right)^3 + a_4 \left(\frac{50}{f} \right)^4 \cdot \left(\frac{Q_{ESP}}{Q_{max}} \right)^4 \tag{10}$$

where a_0, \dots, a_4 —polynomial coefficients, units; Q_{max} —theoretically possible maximum pump flow, m^3/day .

The coefficients of the efficiency polynomials of some ESPs used at oil production enterprises are presented in Table 1 [21].

Table 1. ESP efficiency polynomials.

Nameplate Pump Flow (m^3/Day)	Polynomial Coefficients					Q_{max} (m^3/Day)
	a_0	a_1	a_2	a_3	a_4	
35	−0.00024	0.98450	1.86770	−5.38880	2.55150	68
50	0.00069	1.34660	0.49400	−3.21960	1.37620	98
60	−0.00441	1.81270	−0.23110	−2.54010	0.94720	107

The parameters of the SEM equivalent circuit are determined by the formulas [20,22]:

$$r_{SEM} = \frac{U_{np} \cdot \left(-0.866 \cdot K_L^2 + 1.694 \cdot K_L + 0.156 \right) \cos \varphi_{np}}{\left(0.311 \cdot K_L^2 + 0.226 \cdot K_L + 0.456 \right) \cdot I_{np}} \quad (11)$$

$$r_{SEM} = \frac{U_{np} \cdot \left(-0.866 \cdot K_L^2 + 1.694 \cdot K_L + 0.156 \right) \cos \varphi_{np}}{\left(0.311 \cdot K_L^2 + 0.226 \cdot K_L + 0.456 \right) \cdot I_{np}} \quad (12)$$

where U_{np} is the nameplate voltage of the motor (V); I_{np} —nameplate current of the motor (A); $\cos \varphi_{np}$ —nameplate power factor of the motor (p.u.).

The motor load factor is determined by the formula:

$$K_L = \frac{P_{ESP}}{P_{np}} \quad (13)$$

where P_{np} is the motor nameplate power (W).

The equivalent circuit parameters of an induction motor with a deviation of the voltage at its terminals from the nameplate value are determined by the formulas:

$$r_{SEM.U} = r_{SEM} \cdot \left(\frac{U_{mode}}{U_{np}} \right)^2 \cdot \left(\frac{\cos \varphi_U}{\cos \varphi_{SEM}} \right)^2, \quad (14)$$

$$x_{SEM.U} = x_{SEM} \cdot \left(\frac{U_{mode}}{U_{np}} \right)^2 \cdot \frac{\sin \varphi_{SEM}}{\sin \varphi_U} \cdot \frac{\cos \varphi_U}{\cos \varphi_{SEM}}, \quad (15)$$

where U_{mode} is the mode voltage at the motor terminals (V); $\cos \varphi_{SEM}$ is the motor power factor at a load different from the nameplate (p.u.); the values $\sin \varphi_{SEM}$, $\sin \varphi_U$ are obtained from the basic trigonometric identity.

The motor power factor at different load and voltage at the terminals, different from the nameplate, is calculated by the formula [22,23]:

$$\cos \varphi_U = \cos \varphi_{SEM} \cdot K_{\cos \varphi}, \quad (16)$$

The correction factor is calculated by the expression:

$$K_{\cos \varphi} = \left(-1.6001 + 1.4656 \cdot K_L + 0.7753 \cdot K_L^2 - 0.9114 \cdot K_L^3 \right) \cdot U_{p.u.} + \left(2.6152 - 1.5233 \cdot K_L - 0.7248 \cdot K_L^2 + 0.8974 \cdot K_L^3 \right), \quad (17)$$

The relative voltage at the motor terminals is determined by the formula:

$$U_{p.u.} = \frac{U_{mode}}{U_{np}}, \quad (18)$$

The motor efficiency is described by a polynomial:

$$\eta_{SEM} = \left(0.659 \cdot K_L^4 - 0.367 \cdot K_L^3 - 1.836 \cdot K_L^2 + 2.288 \cdot K_L + 0.259 \right) \cdot \eta_{SEMnp}, \quad (19)$$

where η_{SEMnp} —nameplate motor efficiency (p.u.).

Motor losses are determined by the formula:

$$\Delta P_{SEM} = P_{ESP} \cdot \left(\frac{1}{\eta_{SEM}} - 1 \right), \quad (20)$$

SEM active power is defined as:

$$P_{SEM} = \frac{U_{mode}^2}{|Z_{SEM,U}|} \cdot \cos \varphi_U, \quad (21)$$

where $|Z_{SEM,U}|$ —complex impedance module of the SEM equivalent circuit (Ohm).

The parameters of the equivalent circuit of the cable line are calculated as:

$$r_{CL} = r_0 \cdot l_{CL} \cdot (1 + \alpha(T - 20)), \quad (22)$$

$$x_{CL} = x_0 \cdot l_{CL} \cdot \frac{f}{50}, \quad (23)$$

where r_0, x_0 —specific active and reactive impedances of power lines (Ohm / km); l_{CL} —the length of the cable line (km); α —temperature coefficient of electrical impedance (p.u.); T —the average temperature of the cable cores, ($^{\circ}\text{C}$) (in this case, it is taken in accordance with the average temperature increment in the lithosphere in the amount of ($30^{\circ}\text{C}/\text{km}$)); f —the frequency of the supply voltage (Hz).

The transformer equivalent circuit parameters are calculated as:

$$r_T = \frac{\Delta P_{SC} \cdot U_{HV}^2}{S_{np}^2} \cdot \left(1 - \frac{D}{2} \cdot \frac{St}{100}\right), \quad (24)$$

$$x_T = \sqrt{\left(\frac{U_{SC} \cdot U_{HV}^2}{100 \cdot S_{np}}\right)^2 - r_T^2} \cdot \frac{f}{50} \cdot \left(1 - \frac{D}{2} \cdot \frac{St}{100}\right), \quad (25)$$

where ΔP_{SC} is the nameplate value of the active power losses of the transformer (W); U_{HV} —the nameplate value of the voltage of the transformer high voltage winding (V); S_{np} —transformer rated power (VA); D —discreteness of one stage of voltage regulation (%); St is the number of the selected regulation step (“0” step corresponds to the nominal transformation ratio, steps with “+” —increase the voltage on the low voltage side, steps with “−” —correspond to a decrease in voltage on the low voltage side); U_{SC} —nameplate value of short-circuit voltage (%).

Power losses in a transformer are defined as:

$$\Delta P_T = \Delta P_I + \Delta P_{SC} \cdot \left(\frac{(P_{SEM} + \Delta P_{CL})^2 + (P_{SEM} \cdot \text{tg}(\arccos \varphi_U) + \Delta Q_{CL})^2}{S_{np}^2}\right). \quad (26)$$

The transformation ratio is defined as:

$$K_T = \frac{U_{HV}}{U_{LV}} \cdot \left(1 - \frac{D}{2} \cdot \frac{St}{100}\right). \quad (27)$$

The power loss in the control station is defined as:

$$\Delta P_{CS} = (P_{SEM} + \Delta P_{CL} + \Delta P_T) \cdot (1 - \eta_{CS}), \quad (28)$$

where η_{CS} is the nameplate value of the control station efficiency (p.u.) [24].

2.2.4. Assessment of Harmonics Influence on Electrical Losses

There are various approaches to assess the losses caused by the influence of harmonics, the analysis of which is given in [10,12].

Additional losses in cable lines caused by the influence of harmonics are defined as:

$$\Delta P_{\Sigma vCL} = 3 \cdot \sum_{v=2}^n I_v^2 r_{CL} k_{rv}, \quad (29)$$

where ν is the number of the harmonic; n is the number of harmonics taken into account; I_ν —current of the ν -th harmonic (A); r_{CL} —cable line resistance (Ohm); $k_{r\nu}$ —coefficient, taking into account the influence of the surface effect. As a rule, it is taken equal $k_{r\nu} = 0.47(\nu)^{1/2}$ [12].

Additional losses in the transformer caused by the influence of harmonics are determined as [12]:

$$\Delta P_{\Sigma\nu T} = \Delta P_I \sum_{\nu=2}^n \left(\frac{U_\nu}{U_{HV}} \right)^2 + 0.607 \frac{\Delta P_{SC}}{U_{SC}^2} \sum_{\nu=2}^n \frac{1 + 0.05\nu^2}{\nu\sqrt{\nu}} \left(\frac{U_\nu}{U_{HV}} \right)^2, \quad (30)$$

where U_ν —the voltage of the ν -th harmonic (V).

Additional losses in IM caused by the influence of harmonics are defined as [12]:

$$\Delta P_{\Sigma\nu IM} = k_{IM} P_{np} \sum_{\nu=2}^n \left(\frac{U_\nu}{U_{np}} \right)^2 \left(\frac{\sqrt{\nu} + \sqrt{\nu \pm 1}}{\nu^2} \right), \quad (31)$$

where P_{np} —the nameplate power of the motor (W); U_{np} —nameplate voltage of the motor (V); k_{IM} —coefficient taking into account the parameters of the induction motor; the “+” sign in the radical expression corresponds to the symmetric components of the harmonics rotating against the rotation of the fundamental harmonic field, the “-” sign—to the symmetric components of the harmonics that create the fields, the rotation of which coincides with the rotation of the fundamental harmonic field.

$$k_{IM} = \frac{r_1 I_s^2}{\eta_{np} \cos \varphi_{np}}, \quad (32)$$

where r_1 is the resistance of IM (p.u.); I_s —the multiplicity of the IM starting current (p.u.); η_{np} —the nominal efficiency of the IM (p.u.); $\cos \varphi_{np}$ —nameplate motor power factor (p.u.).

The algorithm for calculating losses in the ETC ESP elements, taking into account the influence of harmonics, is shown in Figure 4.

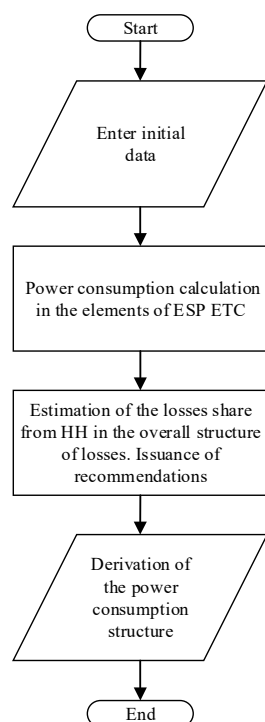


Figure 4. Algorithm for calculating losses in ESP ETC elements, taking into account the influence of harmonics.

3. Results

3.1. Modeling of Power Consumption of ESP as Part of OF ETC

This investigation is a generalization and addition to the research carried out within the project framework [19,22,25] and it has great practical importance in calculating the steady-state modes of electric networks of oil fields.

The block diagram of the OF ETC is proposed, which defines it as an interconnected set of electrical, electromechanical, and hydromechanical subsystems with an emphasis on controlled and observed parameters in each subsystem. The original scheme of interaction ETC ESP elements and the original approach to determining the parameters of the submersible motor equivalent circuit according to the catalog load characteristics are proposed.

A mathematical dependence of the submersible pump efficiency on the electrical and technological modes parameters has been developed (taking into account that the shape of the efficiency curve differs from a parabola, and the point of maximum flow, as a rule, is shifted from the center of the characteristic and does not always correspond to the nominal flow of the pump). The developed method for calculating power consumption makes it possible to take into account the mutual influence of equipment on power consumption within an oil field when changing the technological process parameters.

An assessment was made of the power consumption modeling data of the ESP unit, with the data obtained as a result of instrumental measurements at the wells of the “LUKOIL-PERM” LLC (Perm Territory, Russia).

The values of technological parameters used in modeling are presented in Table 2.

Table 2. Values of technological parameters used in simulation.

#Well	Q_{ESP} (m ³ /day)	H_{dyn} (m)	P_{WH} (MPa)	ρ_1 (kg/m ³)
115	57.7	764	1.4	891
119	57.1	741	2.4	840
120	64.2	750	2.6	839
318	67.0	908	1.5	846

The results of measurements, the results of modeling power consumption, and the results of the error assessment at the selected objects at a voltage of 0.4 (kV) are presented in Table 3.

Table 3. Results of measurements and modeling of ESP power consumption.

#Well	Parameter	Measurement Value	Calculated Value	Relative Error δ (%)
115	Consumption	686.4	648.0	5.6
119	of active	453.6	480.0	5.8
120	energy	919.2	895.2	2.6
318	(kW·h/day)	775.2	700.8	9.6
115	Consumption	504.0	552.0	9.5
119	of reactive	146.4	156.0	6.6
120	energy,	638.4	696.0	9.0
318	(kVAr·h/day)	612.0	648.0	5.9

The mutual influence of equipment within the oil field was taken into account through the nodal voltages when calculating the parameters of power consumption.

3.2. Results of Assessing the Influence of Harmonics on Electrical Losses

Therefore, for example, in the well #115 of the “LUKOIL-PERM” LLC oil field, powered by CTP-2310, installed equipment had the following parameters:

1. SEM: $P_{np} = 40$ (kW); $I_s = 7$; $\eta_{np} = 0.842$; $\cos \varphi_{np} = 0.83$;
2. CL: $L = 2.02$ (km); $r_0 = 1.32$ (Ohm/km);

3. Transformer: $S_{np} = 100$ (kVA); $\Delta P_I = 0.5$ (kW); $\Delta P_{SC} = 2.6$ (kW); $U_{SC} = 5.5$ (%).

The values of the currents and voltages harmonic used in the calculation are presented in Table 4. The measurements were carried out at the outputs of the control station after frequency conversion.

Table 4. The values of the currents and voltages harmonic.

Harmonic Number ν	U_ν (%)	I_ν (%)	Harmonic Number ν	U_ν (%)	I_ν (%)	Harmonic Number ν	U_ν (%)	I_ν (%)
1	100.00	100.00	22	1.92	0.00	43	1.98	0.00
2	7.38	1.07	23	3.80	0.00	44	1.33	0.00
3	0.39	1.38	24	1.01	0.00	45	1.52	0.00
4	8.13	0.88	25	3.12	0.00	46	1.24	0.00
5	6.30	3.52	26	1.08	0.00	47	0.91	0.00
6	2.60	0.48	27	1.01	0.00	48	1.13	0.00
7	4.44	1.02	28	1.59	0.00	49	1.86	0.00
8	7.45	0.26	29	4.74	0.00	50	0.59	0.00
9	0.91	0.00	30	0.83	0.00	51	2.08	0.00
10	6.70	0.00	31	2.56	0.00	52	1.02	0.00
11	16.67	0.97	32	1.09	0.00	53	1.59	0.00
12	1.75	0.00	33	0.67	0.00	54	1.13	0.00
13	15.09	0.49	34	0.35	0.00	55	3.05	0.00
14	4.65	0.00	35	1.34	0.00	56	0.73	0.00
15	0.85	0.00	36	0.56	0.00	57	1.64	0.00
16	4.87	0.00	37	1.15	0.00	58	2.00	0.00
17	6.52	0.33	38	0.98	0.00	59	0.90	0.00
18	1.23	0.00	39	0.79	0.00	60	0.93	0.00
19	3.00	0.00	40	0.81	0.00	61	1.48	0.00
20	2.43	0.00	41	1.62	0.00	62	1.78	0.00
21	1.21	0.00	42	0.93	0.00	63	0.77	0.00

The calculation, without taking into account the influence of the harmonics, was carried out according to Formulas (1)–(28), the calculation taking into account the influence of the harmonics was carried out according to the Formulas (1)–(28) and (29)–(32), and the calculation results are presented in Table 5.

Table 5. Structure of power losses in ESP ETC elements.

Calculation Conditions	Element Loss (kW)				
	ΔP_{ESP}	ΔP_{SEM}	ΔP_{CL}	ΔP_T	ΔP_{CS}
Without taking into account the harmonics influence	13.700	4.520	4.200	1.520	0.920
Taking into account the harmonics influence	13.700	4.786	4.214	1.574	0.920
Additional losses caused by the harmonics influence	0.000	0.266	0.014	0.054	0.000

4. Discussion

Taking into account the structure of the electrotechnical complex of the oil producing enterprise, as well as the list of available initial data, a calculation method was chosen, the initial parameters for which are the powers at the load nodes and the voltage of the substation low voltage buses.

A mathematical dependence of the electric submersible pump efficiency on the parameters of the electric and technological modes has been developed (taking into account that the shape of the efficiency curve differs from the parabola, and the point of maximum flow, as a rule, is shifted from the center of the characteristic and does not always correspond to the nominal pump flow).

Modeling of power consumption of ESP units operating as part of OF ETC was carried out. The simulation results show that the calculation error in comparison with the results

of instrumental measurements is no more than 10%. When modeling power consumption, an analysis of the mutual influence of electric submersible pump installations was carried out. As a result of the analysis, it was revealed that the magnitude of the change in the power consumption parameters, considering the mutual influence of installations, is less than the calculation error.

According to the results of calculations, it was revealed that harmonics have a certain effect on the amount of electricity losses in the ETC of the ESP, and the greatest increase in losses from harmonics is observed in an induction motor. However, it should be noted that in order to assess the increase the elements losses of the ESP ETC from the harmonics, it is necessary to have a composition of harmonic components for each change in the mode, which seems to be difficult to implement. Considering that the losses from the influence of the harmonics are much less than the total losses in all elements of the ESP ETC (including the pump), they can be neglected.

The research results can be used by oil-extracting industry enterprises to assess the amount of power consumption of electric submersible pump installations when changing the technological process parameters, as well as when planning material support and optimizing warehouse stocks within the framework of integrated logistic support for the technological process of industrial enterprises.

Author Contributions: Conceptualization, A.L. and A.P.; methodology, A.R., E.P. and S.M.; software, S.M. and S.Z.; validation, A.K. (Andrei Kokorev) and A.K. (Aleksandr Kokorev); formal analysis, A.L., A.P., A.R. and S.M.; writing—original draft preparation, S.M.; writing—review and editing, A.P. and A.R.; visualization, A.L. and A.P.; supervision, A.P. and A.R. All authors have read and agreed to the published version of the manuscript.

Funding: This research was carried out with the financial support of the Ministry of Science and Higher Education of the Russian Federation in the framework of the program of activities of the Perm Scientific and Educational Center “Rational Subsoil Use”.

Institutional Review Board Statement: Not applicable.

Informed Consent Statement: Not applicable.

Data Availability Statement: Not applicable.

Conflicts of Interest: The authors declare no conflict of interest.

References

1. Brill, J.P.; Mukherjee, H. *Multiphase Flow in Wells*; Henry L. Doherty Memorial Fund of AIME, Society of Petroleum Engineers: Richardson, TX, USA, 1999; 149p.
2. Guo, B.; Lyons, W.C.; Ghalambor, A. *Petroleum Production Engineering. A Computer-Assisted Approach*; Elsevier Science & Technology Books: Amsterdam, The Netherlands, 2007; 287p, ISBN 0750682701.
3. Takacs, G. *Electrical Submersible Pumps Manual: Design, Operations, and Maintenance*; Gulf Professional Publishing: Burlington, MA, USA, 2009; 440p.
4. Liang, X.; Fleming, E. Electrical submersible pump systems: Evaluating their power consumption. *IEEE Ind. Appl. Mag.* **2013**, *19*, 46–55. [[CrossRef](#)]
5. Zhao, Y.; Zhao, D.; Zhong, Y.; Zhao, Y. The Viscosity of Oil Influence on the Working Characteristics of Electric Submersible Pump under Variable Speed. In Proceedings of the 2nd International Conference on Energy, Power, Environment and Computer Application, Beijing, China, 22–23 November 2020. [[CrossRef](#)]
6. Sukhanov, A.; Gansheng, A.Y.; Jichao, Y.; Perelman, O.; Derkach, N. Enhancement of Electric Submersible Pump Energy Efficiency by Replacing an Inductive Motor with a Permanent Magnet Motor. *Oil Gas Eur. Mag.* **2020**, *3*, 146–150. [[CrossRef](#)]
7. Leon, J.L.V.; Ruales, F.; Miranda, S.; Godin, F.; Velasquez, E.; Shirikov, D.; Anaya, O.; Forero, N.; Estupiñan, N.D.; Peña, L.; et al. Permanent Magnet Motors: The Future of ESP Applications? In Proceedings of the SPE Gulf Coast Section Electric Submersible Pumps Symposium, Virtual. The Woodlands, TX, USA, 4–8 October 2021. [[CrossRef](#)]
8. Alexeev, Y.; Shakirov, A.; Yamilov, R. Challenges and Results of the First Ultra-High-Speed ESP Rental Project—A Case Study. Hyper Speed ESP 15,000 rpm as the Next Step to the Future. In Proceedings of the SPE Gulf Coast Section Electric Submersible Pumps Symposium, Virtual. The Woodlands, TX, USA, 4–8 October 2021. [[CrossRef](#)]
9. Khakim'yanov, M.I. Investigation of Power Loss in the Cable of a Well Submersible Motor. *Russ. Electr. Eng.* **2018**, *2*, 103–106. [[CrossRef](#)]

10. Abramov, B.I.; Parfenov, B.M.; Shevyrev, Y.V. Choice Methods of the Parameters of Filter Compensating Stepped Type Devices for Thyristor Electric Drives. *Elektrotehnika* **2001**, *1*, 38–42.
11. Dems, M.; Komeza, K.; Majer, K. Core Losses of the Induction Motor Operating in A Wide Frequency Range Supplied from the Inverter. *Int. J. Appl. Electromagn. Mech.* **2020**, *64*, S65–S82. [[CrossRef](#)]
12. Otcenasova, A.; Bolf, A.; Altus, J.; Regula, M. The influence of power quality indices on active power losses in a local distribution grid. *Energies* **2019**, *12*, 1389. [[CrossRef](#)]
13. Li, L.; Huang, H.; Zhao, F.; Gao, M.; Liu, Z.J.W. Sutherland Power measurement in energy efficient manufacturing: Accuracy analysis, Challenges, and Perspectives for improvement. In Proceedings of the 26th CIRP Conference on Life Cycle Engineering, LCE 2019, West Lafayette, IN, USA, 7–9 May 2019. [[CrossRef](#)]
14. Romanska-Zapala, A.; Dechnik, M.; Grzywocz, K. Power Quality in Energy Efficient Buildings-A Case Study. In Proceedings of the 4th World Multidisciplinary Civil Engineering-Architecture-Urban Planning Symposium, WMCAUS 2019, Prague, Czech Republic, 17–21 June 2019. [[CrossRef](#)]
15. Derendiaeva, L.V.; Zakalata, A.A.; Ojegov, A.N. Application of equivalent method for electric power grid subsystems in calculating the higher harmonics mode. In Proceedings of the 2017 International Conference on Industrial Engineering, Applications and Manufacturing, ICIEAM 2017, Chelyabinsk, Russia, 16–19 May 2017. [[CrossRef](#)]
16. Lyutarevich, A.G.; Vyrva, A.A.; Dolinger, S.Y.; Osipov, D.S.; Chetverik, I.N. Ocenka Dopolnitel'nyh Poter' Moshchnosti Ot Vysshih Garmonik V Elementah Sistem Elektrosnabzheniya [Assessment of Additional Power Losses from Higher Harmonics in The Elements of Power Supply Systems]. *Omskij Nauchnyj Vestnik* **2009**, *1*, 109–113. (In Russian)
17. Gevorkov, L.; Rassolkin, A.; Kallaste, A.; Vaimann, T. Simulation Study of a Centrifugal Pumping Plant's Power Consumption at Throttling and Speed Control. In Proceedings of the 2017 IEEE 58th International Scientific Conference on Power and Electrical Engineering of Riga Technical University (RTUCon), Riga, Latvia, 12–13 October 2017; pp. 1–5. [[CrossRef](#)]
18. Gevorkov, L.; Šmidl, V. Simulation Model for Efficiency Estimation of Photovoltaic Water Pumping System. In Proceedings of the 2020 19th International Symposium INFOTEH-JAHORINA (INFOTEH), East Sarajevo, Bosnia and Herzegovina, 18–20 March 2020; pp. 1–5. [[CrossRef](#)]
19. Petrochenkov, A.; Romodin, A.; Mishurinskikh, S.; Speshilov, P. Development of the Oil Well Electrotechnical Complex Model in LabVIEW: Application work package. In Proceedings of the 8th International Conference on Applied Innovation in IT, Koethen, Germany, 10 March 2020. [[CrossRef](#)]
20. Petrochenkov, A.B.; Mishurinskikh, S.V. Development of a Method for Optimizing Power Consumption of an Electric Driven Centrifugal Pump. In Proceedings of the 2021 IEEE Conference of Russian Young Researchers in Electrical and Electronic Engineering (ElConRus), St. Petersburg, Russia, 26–29 January 2021. [[CrossRef](#)]
21. Standard ESP Systems. Available online: <https://www.novometgroup.com/products-services/artificial-lift/electrical-submersible-pumping-systems/standard-esp> (accessed on 15 January 2022).
22. Petrochenkov, A.B.; Romodin, A.V.; Mishurinskikh, S.V.; Seleznev, V.V.; Shamaev, V.A. Experience in Developing a Physical Model of Submersible Electrical Equipment for Simulator Systems: Research and Training Tasks on the Agenda of a Key Employer. In Proceedings of the 2018 XVII Russian Scientific and Practical Conference on Planning and Teaching Engineering Staff for the Industrial and Economic Complex of the Region, St. Petersburg, Russia, 14–15 November 2018. [[CrossRef](#)]
23. Mishurinskikh, S.V.; Petrochenkov, A.B. Metodicheskie rekomendacii po ocenke reaktivnoj moshchnosti, potrebyaemoj pogrzhnym asinhronnym elektrodvigatelem [Guidelines for Assessing the Reactive Power Consumed by a Submersible Induction Motor]. *Vestnik PNIPU* **2021**, *38*, 175–194. (In Russian) [[CrossRef](#)]
24. Kalinin, Y.; Chivenkov, A.; Vagapov, Y.; Anuchin, A. Determining Specific Power Loss in Joint Area of Laminated Magnetic Core. In Proceedings of the 2021 28th International Workshop on Electric Drives: Improving Reliability of Electric Drives (IWED), Online. 27–29 January 2021. [[CrossRef](#)]
25. Petrochenkov, A.B. Regarding Life-Cycle Management of Electrotechnical Complexes in Oil Production. *Russ. Electr. Eng.* **2012**, *83*, 621–627. [[CrossRef](#)]